ORIGINAL PAPER

Overstepping the garnet isograd: a comparison of QuiG barometry and thermodynamic modeling

Frank S. Spear · Jay B. Thomas · Benjamin W. Hallett

Abstract The consequences of overstepping the garnet isograd reaction have been investigated by comparing the composition of garnet formed at overstepped P–T conditions (the overstep or "OS" model) with the P–T conditions that would be inferred by assuming garnet nucleated in equilibrium with the matrix assemblage at the isograd (the equilibrium or "EQ" model). The garnet nucleus composition formed at overstepped conditions is calculated as the composition that produces the maximum decrease in Gibbs free energy from the equilibrated, garnet-absent, matrix assemblage for the bulk composition under study. Isopleths were then calculated for this garnet nucleus composition assuming equilibrium with the matrix assemblage (the EQ model). Comparison of the actual P–T conditions of nucleation (the OS model) with those inferred from the EQ model reveals considerable discrepancy between the two. In general, the inferred garnet nucleation P–T conditions (the EQ model) are at a lower temperature and higher or lower pressure (depending on the coexisting calcic phase(s)) than the actual (OS model) nucleation conditions. Moreover, the degree of discrepancy increases with the degree of overstepping. Independent estimates of the pressure of nucleation of garnet were made using the Raman shift of quartz inclusions in garnet (quartz-in-garnet or QuiG barometry). To test the validity of this method, an experimental synthesis of garnet containing quartz inclusions was made at 800 °C, 20 kbar, and the measured Raman shift reproduced the synthesis conditions to within 120 bars. Raman band shifts from three natural samples were then used to calculate an isochore along which garnet was presumed to

have nucleated. Model calculations were made at several temperatures along this isochore (the OS model), and these P–T conditions were compared to those computed assuming equilibrium nucleation (the EQ model) to estimate the degree of overstepping displayed by these samples. A sample from the garnet isograd in eastern Vermont is consistent with overstepping of around 10 degrees and 0.6 kbar (affinities of around 2 kJ/mole garnet). A sample from the staurolite–kyanite zone in the same terrane requires overstepping of around 50 °C and 2–5 kbar (affinities of around 10–18 kJ/mole garnet). A similar amount of overstepping was inferred for a blueschist sample from Sifnos, Greece. These results indicate that overstepping of garnet nucleation reactions may be common and pronounced in regionally metamorphosed terranes, and that the P–T conditions and paths inferred from garnet zoning studies may be egregiously in error.

Keywords Raman spectroscopy · Overstepping · Garnet isograd · QuiG barometry · Quartz inclusions · P–T conditions

Introduction

Nucleation of an index mineral such as garnet requires sufficient overstepping of the isograd reaction to overcome the nucleation barrier. Although the necessity of some degree of overstepping is given, the amount of overstepping required to nucleate a phase such as garnet is poorly known. Pattison et al. (2011; see also Gaidies et al. 2011) presented a thorough evaluation of the available energies (affinities) as a function of overstepping for a number of important index mineral reactions and suggested a number of significant petrologic consequences for overstepping isograd reactions. Indeed, depending on the setting and model assumptions,

F. S. Spear (✉) · J. B. Thomas · B. W. Hallett
Department of Earth and Environmental Sciences, Rensselaer Polytechnic Institute, Troy, NY 12180, USA
e-mail: spearf@rpi.edu

estimates of the degree of overstepping by numerous authors range from a few degrees to many tens of degrees (e.g., Walther and Wood 1984; Lasaga 1986; Lasaga and Rye 1993; Manning et al. 1993; Waters and Lovegrove 2002; Zeh and Holness 2003; Wilbur and Ague 2006; Pattison and Tinkham 2009; Pattison and Seitz 2012; Gaidies et al. 2011).

Evaluation of the degree of overstepping requires independent means of comparing the expected (equilibrium) isograd P–T conditions with the actual conditions of nucleation. For example, Pattison and Tinkham (2009) have used the spacing of isograds around the Nelson aureole, British Columbia, to infer the delay in the onset of several key prograde reactions in metapelites. Experimental studies (e.g., Ridley and Thompson 1986; Rubie 1998) also provide insights into the behavior of metamorphic systems but are difficult to extrapolate to natural settings and presumed geologic rates.

Raman spectroscopy on quartz inclusions in garnet (i.e., "Geoba-Raman-try": Kohn 2013, 2014; Ashley et al. 2014; Enami et al. 2007; Guiraud and Powell 2006), hereafter referred to as QuiG (Kohn 2013, 2014), provides a means of determining the pressure of garnet formation that is completely independent of assumptions about chemical equilibrium and thus provides a means of comparing the expected (equilibrium) isograd conditions with the actual conditions of garnet nucleation. The method is based on the Raman shift of quartz peaks as a function of pressure. The Raman shift is measured at ambient conditions to yield the pressure on the inclusion. Equations of state for quartz and garnet are coupled to a thermoelastic model to yield the locus of P–T points along which garnet growth trapped the quartz inclusion assuming no post-entrapment non-elastic deformation has occurred (e.g., cracking) (e.g., Ashley et al. 2014).

This paper presents theoretical models of overstepping of the garnet isograd reaction in three samples from regionally metamorphosed terranes: two from the Barrovian terrane of eastern Vermont (samples TM-549 and TM-626) and one from the Cyclades blueschist belt on Sifnos, Greece (sample 06MSF-6C of Dragovic et al. 2012). Following the approach of Pattison et al. (2011) and Gaidies et al. (2011), it is possible to calculate the composition of garnet that would form upon nucleation for any degree of overstepping. This is predicted to be the garnet core composition and will be referred to as the "overstep" (OS) model. The OS model is then compared to the P–T conditions that would be calculated if it were assumed that the garnet nucleated in equilibrium with matrix phases at the garnet isograd. These calculations are made using the method of intersecting garnet core isopleths for the specified whole-rock bulk composition and will be referred to as the "equilibrium" (EQ) model. The results of the two sets of calculations (the P–T conditions of the OS model and those inferred from the EQ model) are then compared to assess the degree to which the inferred P–T conditions from the EQ model might be in error based on assumed

equilibrium. The results, as will be seen, indicate that significant overstepping of the garnet-in reaction would result in egregious mistakes in the inferred P–T path and the tectonic implications drawn from the erroneous path.

Method

Thermodynamic modeling

This study focuses on the composition of the garnet at the instant of nucleation assuming overstepping of the isograd reaction. This is the composition that will form the core of the growing porphyroblast, which is an important point on the P–T path of the rock. There are several possibilities for the composition of the nucleus. (1) The nucleus could have the composition that the phase would have had if it had nucleated when it crossed the isograd (the equilibrium isograd composition). This is not supportable because the compositions of the matrix phases (e.g., chlorite, plagioclase, and biotite) should be different at the overstepped P–T conditions than they were at the isograd, and the partitioning between garnet and the matrix phases at the P–T conditions of nucleation should be different from what they would have been at the isograd. (2) The nucleus could be of a composition that maintains partitioning equilibrium at the overstepped P–T conditions. This option is impossible to achieve for all partitioning equilibria simultaneously unless the matrix minerals change composition spontaneously to the equilibrium compositions. (3) The nucleus could have a composition that maximizes the decrease in free energy of the system. This is the hypothesis proposed by Pattison et al. (2011—their model 3), and it is believed to be the most probable because it maximizes the available free energy to overcome the nucleation barrier.

A G–X diagram that depicts hypothesis (3) (the OS model) is shown in Fig. 1. The composition of garnet at the instant of nucleation can be calculated in the following manner. First, a bulk composition is chosen and the garnet isograd is calculated assuming equilibrium. The P and T of nucleation are then chosen at some arbitrary conditions above the isograd, and the equilibrium compositions of the matrix phases (without garnet) are calculated. It can be seen from Fig. 1 that the condition that maximizes the decrease in free energy is where the tangent to the garnet free energy surface is parallel to the tangent to the matrix assemblage. Parallel tangents require that the slopes be equal or

$$\mu_{alm}^{Grt} - \mu_{prp}^{Grt} = \mu_{alm}^{Matrix} - \mu_{prp}^{Matrix}$$

$$\mu_{sps}^{Grt} - \mu_{prp}^{Grt} = \mu_{sps}^{Matrix} - \mu_{prp}^{Matrix}$$

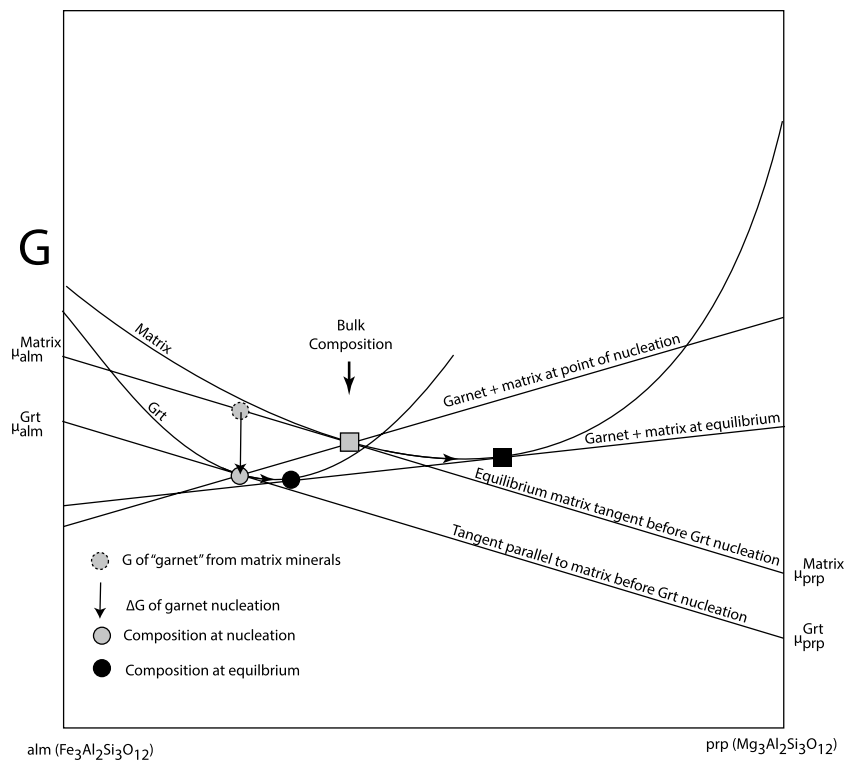$$\mu_{grs}^{Grt} - \mu_{prp}^{Grt} = \mu_{grs}^{Matrix} - \mu_{prp}^{Matrix}$$

Fig. 1 Schematic G–X diagram showing graphically the method used to calculate garnet composition at nucleation. *Squares* are matrix, *circles* are garnet. *Tangent lines* show "Equilibrium matrix tangent before Grt nucleation," the "Tangent (to garnet *G*-surface) parallel to matrix before Grt nucleation," the line (out of equilibrium) at the point of nucleation "Garnet + matrix at point of nucleation," and the "Garnet + matrix at equilibrium" tangent line. *Gray square* on the matrix *G*-surface shows the *G* of the matrix before nucleation

and the *dotted gray circle* shows the *G* of the fictive garnet (not yet nucleated). *Gray circle* along garnet *G*-surface shows the composition of garnet nucleus, and the *arrow* shows the maximum ΔG assumed in this method. *Black circle* and *square* show the eventual equilibrium between garnet and matrix. μ_{alm}^{Grt}, μ_{alm}^{Matrix}, μ_{prp}^{Grt} and μ_{prp}^{Matrix} are the chemical potentials of almandine and pyrope in the garnet and matrix, respectively. *Arrows* along garnet and matrix *G–X curves* show progress toward equilibrium after nucleation

The chemical potentials of the garnet components defined by the matrix phases are calculated as a linear combination of components of matrix phases. For example,

$$\mu_{prp}^{Matrix} = 1.333\mu_{qtz}^{Qtz} + 0.333\mu_{clinochlore}^{Chlorite} + 0.333\mu_{amesite}^{Chlorite} - 2.667\mu_{H_2O}^{Matrix}$$

$$\mu_{alm}^{Matrix} = 1.333\mu_{qtz}^{Qtz} - 0.267\mu_{clinochlore}^{Chlorite} + 0.333\mu_{amesite}^{Chlorite} - 0.6\mu_{daphanite}^{Matrix} - 2.667\mu_{H_2O}^{Matrix}$$

$$\mu_{sps}^{Matrix} = 1.333\mu_{qtz}^{Qtz} + 0.267\mu_{9-6-5Mn-chlorite}^{Chlorite} - 2.667\mu_{H_2O}^{Matrix}$$

$$\mu_{grs}^{Matrix} = 3.667\mu_{qtz}^{Qtz} + 0.3\mu_{anorthite}^{Plagioclase} + 1.333\mu_{clinochlore}^{Chlorite} - 1.667\mu_{amesite}^{Chlorite} + 1.333\mu_{H_2O}^{Matrix}$$

The three independent equations relating the chemical potentials of the garnet and matrix components are solved using Newton's method for the composition of garnet at the point of nucleation. The affinity for nucleation is then calculated as

$$\mu_{prp}^{Grt} - \mu_{prp}^{Matrix} = \mu_{alm}^{Grt} - \mu_{alm}^{Matrix}$$
$$= \mu_{sps}^{Grt} - \mu_{sps}^{Matrix} = \mu_{grs}^{Grt} - \mu_{grs}^{Matrix}$$

The equilibrium model is then applied to the composition of the garnet nucleus to calculate the P–T conditions using the method of intersecting isopleths using the same bulk composition that was used in the OS model. The two sets of P–T conditions are then compared.

All model calculations were done in the MnNCKF-MASH system using modules written for Program Gibbs (e.g., Spear and Menard 1989; Spear et al. 1991) with thermodynamic data from Spear and Pyle (2010).

Raman Spectroscopy

Raman spectra of quartz inclusions in garnet were measured with a Jobin Yvon LabRam HR800 Raman microprobe at Rensselaer Polytechnic Institute. The incident 632.82 nm laser

(20 mW HeNe laser) was focused onto quartz inclusions in garnet using a 100× microscope objective (N.A.=0.9). The Raman light was backscattered (180° geometry) and dispersed using an 1,800 groove/mm grating onto a charged-couple device. Spectra were acquired for 60 s. The confocal hole was adjusted to maximize the signal from quartz inclusions. The zero position of spectra was adjusted using Rayleigh scattered light of the 632.82 nm laser. The 520.7 cm^{-1} band of a silicon chip was used to calibrate spectrometer linearity. The main band in α quartz at about 464 cm^{-1} arises from motions of O in Si–O–Si symmetric stretching-bending vibrations (Hemley 1987). Quartz in the matrix is exposed to ambient pressure; thus, the main band occurs at 464 cm^{-1}. The Si–O–Si band of quartz inclusions is shifted because the garnet host is applying pressure to the inclusion. The Raman shift of the quartz inclusions is reported relative to the 464 cm^{-1} band in the matrix quartz, which was repeatedly measured in each analytical session.

The Raman shifts of the 464 cm^{-1} quartz peak were converted into internal pressures using the calibration of Ashley et al. (2014), which is based on the experimental dataset of Schmidt and Ziemann (2000):

$$P(bar) = 4.204\Delta V^2 + 1094.5\Delta V$$

The pressure of entrapment of the quartz inclusion at a specified temperature was calculated using the thermoelastic model of Guiraud and Powell (2006):

$$P_{incl} = 1 - \frac{4\mu}{3}\left(\frac{V_{host}^{298,1\,bar}}{V_{host}^{T,P}} - \frac{V_{host}^{298,P_{incl}}}{V_{incl}^{T,P}}\right)$$

where μ is the shear modulus for garnet and V is the volume of the host or inclusion at the superscripted conditions. Equations of state and elastic parameters for garnet and quartz are taken from Kohn (2014). Calculations were done over a range of temperatures yielding isochores for quartz entrapment. It is presumed that garnet nucleated at some point along this isochore.

Bulk composition estimation

The P–T conditions of garnet nucleation assuming equilibrium nucleation at the garnet isograd were calculated using an estimated bulk composition and the method of intersecting isopleths. The two samples from Vermont (sample TM-549 and TM-626) are layered so it was not deemed feasible to consider a bulk-rock analysis of the entire sample or even of selected layers of the sample. The bulk composition was therefore estimated in two ways. First, an estimate of the modal amount of garnet was made on the appropriate compositional layers using a scanned image of the polished thin section. The relative modal amounts of muscovite, biotite, chlorite, quartz, K-feldspar, and plagioclase were estimated from

Table 1 Bulk-rock analyses used in calculations

	BC1 (Fig. 2)	TM-549 BC(a)[a]	TM-549 BC(b)[b]	TM-6262	06MSF-6C[c]
SiO2	54.09	55.71	62.96	55.72	53.15
Al2O3	25.53	20.84	17.94	16.16	13.77
Fe2O3	–	–	–	–	4.15
MgO	3.58	3.61	3.67	3.97	5.65
FeO	6.94	6.38	6.38	10.76	9.19
MnO	0.32	0.17	0.20	0.44	0.14
CaO	1.55	0.97	1.32	0.64	2.72
Na$_2$O	0.78	1.80	2.40	1.25	5.30
K$_2$O	5.87	5.81	2.39	4.05	0.99
H$_2$O[d]	5.33	4.72	5.0	6.0	5.0

[a] Composition determined from modal analysis of X-ray maps using ImageJ multiplied by phase composition

[b] Composition determined from average electron microprobe spot analyses with broadened beam

[c] Whole-rock analysis from Dragovic et al. (2012)

[d] Sufficient H$_2$O was added to each bulk composition to ensure excess fluid at all P–T conditions

image analysis of X-ray maps using thresholding to isolate individual phases and then renormalized to include garnet. The bulk composition was calculated by multiplication of the modal amounts by the measured composition of each phase using an average garnet composition determined by volume normalization (Table 1). Method 2 involved averaging electron microprobe spot analysis of matrix minerals (±garnet) within the appropriate compositional layer using a 20-μm defocused beam. For sample TM-549, the bulk composition was calculated by multiplying the average of 450 matrix spot analyses and the average garnet composition by their respective modal amounts (Table 3), and for sample TM-626, the bulk composition was estimated from the average of 1,800 spot analyses.

For sample 06MSF-6C from Sifnos, Greece, the bulk composition was taken as the whole-rock analysis from the study of Dragovic et al. (2012; their Table 2).

Results

Experimental test of QuiG barometry

A single experiment to test the accuracy of QuiG barometry was conducted in the piston cylinder laboratory of E. B. Watson at Rensselaer Polytechnic Institute. An oxide starting mix was recrystallized at 800 °C and 20 kbar in a silver capsule in the presence of excess H$_2$O fluid. The uncertainty in temperature and pressure in this apparatus has been determined to be approximately ±10 °C and ±200 bars (E. B. Watson, personal communication). The

Table 2 Comparison of equilibrium garnet compositions (the EQ model) with nucleation garnet compositions for three model oversteps (the OS model)

	Case 1		Case 2		Case 3	
T&P	534 °C, 4894 bars		584 °C, 4,894 bars		484 °C, 6,393 bars	
Affinity[a]	4,014 J		9,585 J		3,141 J	
	Nucleation	Equilibrium	Nucleation	Equilibrium	Nucleation	Equilibrium
Pyrope	4.69	6.09	6.16	11.84	2.68	3.30
Almandine	55.56	65.10	60.05	73.78	39.77	46.08
Spessartine	30.51	17.73	29.96	8.27	23.61	14.69
Grossular	9.24	11.07	3.82	6.09	33.93	35.92

[a] Affinity is joules/mole of garnet (12 oxygen basis) produced
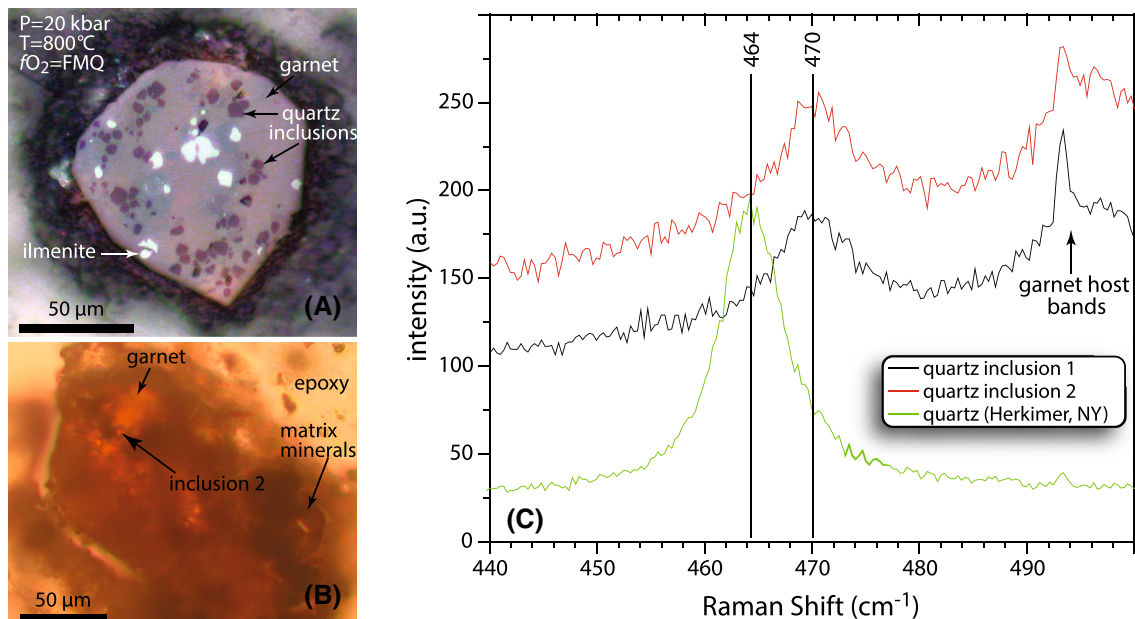
Fig. 2 **a** Reflected light photograph of a garnet crystal synthesized at 20 kbar and 800 °C showing numerous quartz inclusions exposed at the polished surface. **b** Transmitted light photograph of the same garnet crystal showing a quartz inclusion (not exposed) that was meas- ured. **c** Raman spectra of quartz inclusions compared with a quartz standard from Herkimer, NY. The O–Si–O band of quartz inclusions that are contained inside the garnet is shifted to 470 cm^{-1}

oxygen fugacity was controlled by the fayalite–magnetite–quartz buffer assemblage contained in an internal capsule.

Garnet, quartz, ilmenite, and kyanite readily grew during the experiment, and garnet was observed to contain numerous inclusions of quartz (Fig. 2a). The transmitted light photograph in Fig. 2b shows a specific quartz inclusion (not exposed at the surface) that was measured using the Raman microprobe. A standard quartz crystal from Herkimer, NY, was measured before and after every measurement of quartz inclusions to ensure spectral accuracy of the O–Si–O bending band, which occurs at 464 cm^{-1} at $P = 1$ bar. The O–Si–O bending band of the quartz inclusions from the experiments was shifted to 470 cm^{-1} (Fig. 2c). Application of the thermoelastic model described above yields an entrapment pressure at 800 °C of 19.880 kbar—essentially identical to the experimental pressure of 20 kbar. This experiment demonstrates that, in the absence of non-elastic garnet deformation around the inclusion, QuiG barometry should accurately reflect the conditions of entrapment.

Model oversteppping calculations: general results

Calculations have been done with a hypothetical bulk composition (BC1: Table 1) to explore some general behavior of the overstepped system. A partial pseudosection for this bulk composition showing the garnet isograd and contoured for garnet composition is presented in Fig. 3a–c. Contours of reaction affinity (calculated as ΔG of garnet nucleation) (Fig. 3d) were done by iterating on temperature or pressure, depending on the slope of the affinity isopleth, using Newton's method to achieve a contour of the desired amount of affinity.
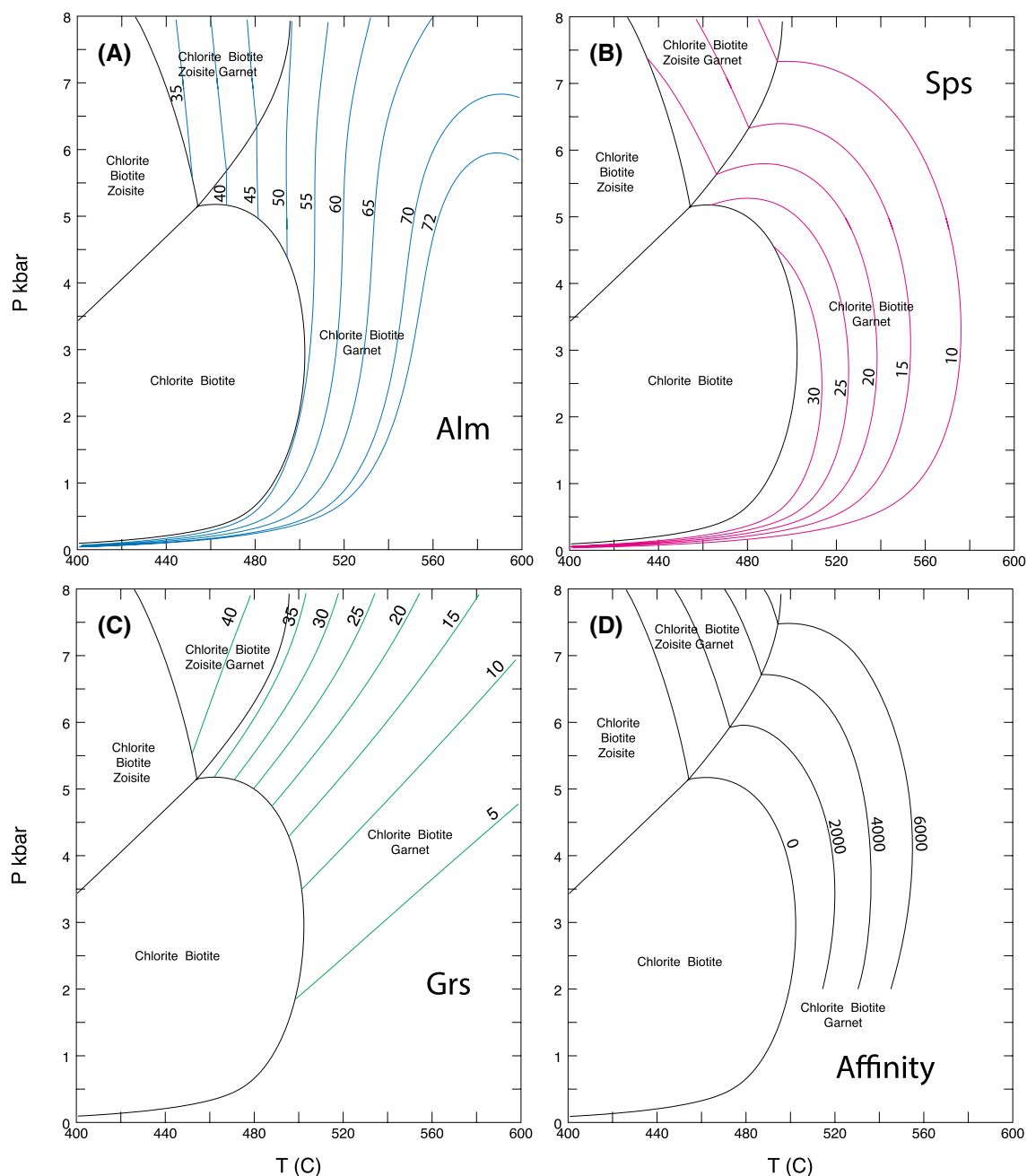
Fig. 3 Partial pseudosection for the bulk composition BC1 (Table 1) contoured for **a** almandine, **b** spessartine, **c** grossular, and **d** affinity. All assemblages contain quartz, muscovite, and fluid

Detailed calculations of garnet composition at the point of nucleation were done for three model P–T points representative of different degrees of overstepping (Fig. 4: circles). For each point, the garnet composition was calculated along with the affinity, and the results are presented in Table 2. For comparison, the equilibrium composition of garnet at the same P–T conditions is also shown for each of the three points. As can be seen, the composition of the nucleating garnet is quite different from the equilibrium composition. For example, Case 1 represents 50° of overstepping and generates an affinity of 4,014 J per mole of garnet (12 oxygens). The composition of garnet at nucleation has mole percent spessartine = 30.51, whereas the equilibrium composition is only 17.73. Other garnet components show different amounts of disparity between the two compositions. Very similar compositional differences were calculated by Gaidies et al. (2011) using a similar method. The magnitude of affinity from these calculations
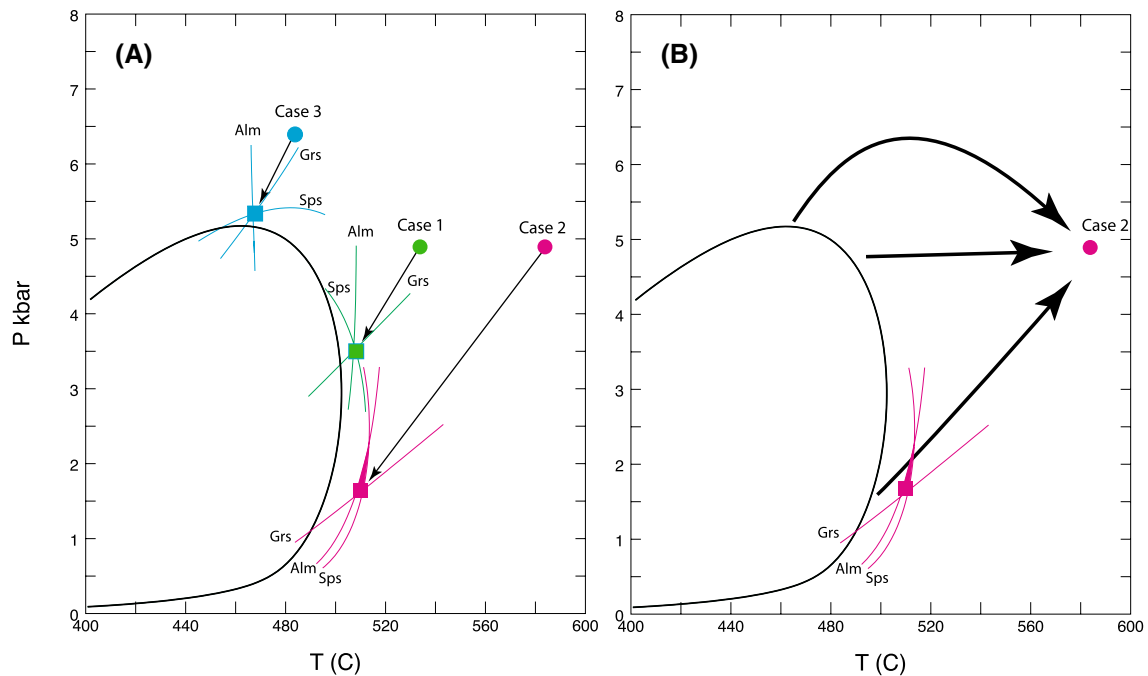
Fig. 4 **a** P–T diagrams showing garnet isograd for BC1 (Table 1). *Case 1*, *2*, and *3* are three different P–T conditions representing three different degrees of overstepping for the calculation of garnet composition at nucleation (the OS model—*circles*). Intersecting isopleths of almandine, spessartine, and grossular using the composition at nucleation (i.e., the garnet core) and assuming nucleation occurred under conditions of equilibrium (the EQ model—*squares*) are shown. Note the difference between the P–T conditions of nucleation (*circles* OS model) and the P–T conditions that would be inferred from assuming nucleation at equilibrium (*squares* and intersecting isopleths: EQ model). *Arrows* link P–T conditions of the OS and EQ models. **b** P–T diagram for *case 2* emphasizing that the true P–T path to the conditions of nucleation is unknown and the degree to which erroneous interpretations might be inferred

is similar, although not exactly identical, to those reported by Pattison et al. (2011, their Fig. 2), Gaidies et al. (2011), and Pattison and Seitz (2012). For example, for the reaction

$$Ms + Chl + Qtz = Grt + Bt + H_2O$$
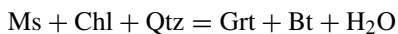
Pattison et al. (2011, Fig. 2) calculated on the order of 10 J/mole O per degree of overstepping. For 50 degrees of overstepping, their plot indicates around 500 J/mole oxygen or 6 kJ per 12 oxygen garnet.

Also shown in Fig. 4a are the P–T conditions calculated from the intersection of almandine, spessartine, and grossular isopleths using the composition of the garnet at the point of nucleation (squares: the EQ model). Each of these three sets of P–T conditions lies at lower temperature and pressure than the true P–T conditions of nucleation owing to the difference in garnet composition of the nucleated core compared with the equilibrium composition (Table 2). For example, the P–T conditions of garnet nucleation for Case 1 are 534 °C, 4,894 bars, whereas the P–T conditions inferred from the intersecting isopleths assuming no overstepping are 508 °C, 3,500 bars. In general, the discrepancy increases as a function of the affinity for nucleation. The principal reason for the lower temperature and pressure is

the lower spessartine and grossular contents of the overstepped garnet core relative to the equilibrium compositions (Table 2).

It is also interesting to note that there is good intersection of the three independent garnet isopleths, although the error of intersection appears to increase with increasing affinity. Therefore, it is clear that good intersection of the isopleths is not a reliable criterion for the garnet core having crystallized at or near equilibrium. Somewhat surprisingly, the intersecting isopleth P–T conditions fall near the equilibrium garnet isograd, and it may also be concluded that proximity to the equilibrium isograd is not a good criterion for the assessment of equilibrium.

As Fig. 4a clearly illustrates, overstepping the garnet nucleation reaction can result in significant errors in the presumed P–T conditions of nucleation of the garnet core. If an approach to equilibrium is finally achieved at the garnet rim so accurate P–T conditions are available for the rim, then the inferred P–T path for the sample could be egregiously in error. In particular, there is no information available in the garnet about the path the sample followed to attain the P–T conditions of nucleation, so the path along this part of the rock's history is completely unconstrained. As an example, the P–T path followed by a rock

represented by Case 2 might have followed any number of trajectories (e.g., Figure 4b). Clearly, the tectonic inferences drawn from the P–T paths in Fig. 4b would be quite different. It must be concluded that the degree of overstepping is critical to evaluate before accurate P–T paths can be inferred from garnet zoning.

Model overstepping calculations: natural samples

The model calculations presented above are limited because there is no independent means to determine the conditions of garnet nucleation. Natural samples with appropriate inclusions of quartz in garnet are amenable to the calculation of a P–T line along which garnet formed by the application of the QuiG (quartz-in-garnet) barometer (Enami et al. 2007; Ashley et al. 2014; Kohn 2013, 2014).

Garnet isograd, Eastern Vermont: Sample TM-549

Sample TM-549 is from the garnet isograd in Eastern Vermont. Aspects of the paragenesis of this sample were discussed by Menard and Spear (1994) who inferred peak P–T conditions of 460–500 °C, 4–5 kbar from thermobarometry. The reader is referred to that paper for sample location and further details of the general geologic setting. A photomicrograph and X-ray maps for the largest garnet from sample TM-549 are shown in Fig. 5, and the measured garnet core composition is listed in Table 3. The garnet is approximately 1.5 mm in diameter and overgrows an incipient crenulation cleavage. X-ray maps (Fig. 5) and a line traverse (Fig. 6) reveal only minor zoning of almandine, spessartine, and grossular. Core-to-rim compositional variation is $X_{prp} = 5.77–5.33$; $X_{alm} = 53.80–57.41$; $X_{sps} = 29.24–25.17$; $X_{grs} = 11.19–12.07$.

The Raman shift of the 464 cm^{-1} peak of twelve quartz inclusions in two garnets was measured (Table 4; Fig. 7a). The inclusions displayed Raman shifts in the range from -0.1 to 1.3 cm^{-1} (± 0.1). Any non-elastic deformation of the host garnet in the vicinity of the quartz inclusion can lead to a reduction in the internal pressure on the quartz inclusion. Therefore, only the grains that display the maximum Raman shift are believed to reflect the conditions of quartz entrapment. Several grains show shifts of 1.1–1.3 (± 0.1) cm^{-1}, which corresponds to an internal pressure on quartz of 1,209–1,430 bars.

The two bulk compositions for sample TM-549 in Table 1 were used to calculate the garnet isograd (Fig. 8a) as well as isopleths for almandine, spessartine, and grossular using the composition of the garnet core (Table 3; Fig. 8a). The two bulk compositions differ slightly, and
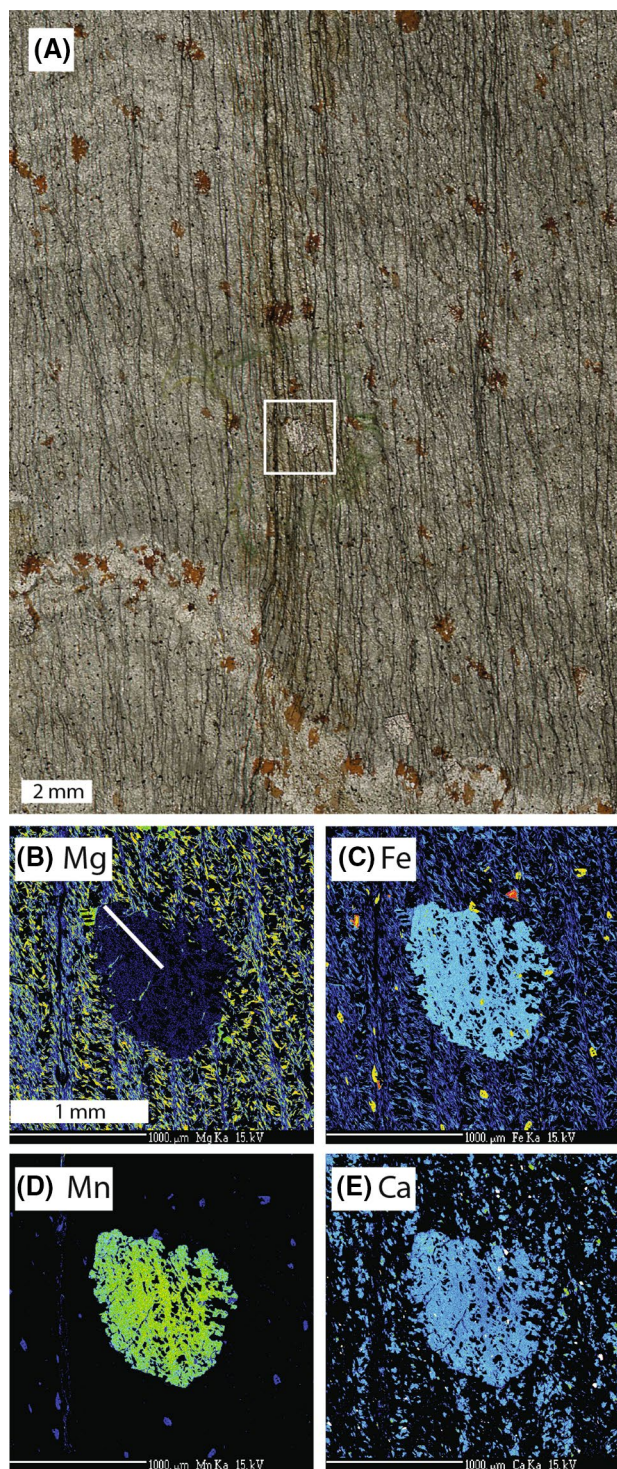

Fig. 5 Sample TM-549 (Latitude = 43.79510; Longitude = −72.28250). **a** Photomicrograph. **b**–**e** X-ray maps of **b** Mg; **c** Fe; **d** Mn; and **e** Ca. Note that garnet is small, overgrows a crenulation cleavage, and is only weakly zoned. *Box* in (**a**) shows the location of garnet X-ray maps. *White line* in (**b**) shows the location of traverse in Fig. 6

the small difference in the location of the garnet isograd is due to the minor difference in MnO content (0.17 versus 0.20 wt%). The two sets of intersecting isopleths yield nearly identical P and T (Fig. 8a) and correspond nearly exactly with the equilibrium garnet isograd for bulk composition BC(b). The isopleth pressures are, however, approximately 600 bars below the pressure inferred from the QuiG barometry.

The difference between the thermodynamic calculation (the EQ model) and the entrapment pressure from the Raman measurement is similar in direction to the variation expected assuming a small amount of overstepping (e.g., Case 1, Fig. 4b). To provide additional quantification, further calculations were performed using the bulk compositions BC(a) and BC(b) for TM-549 at five P–T conditions along the quartz inclusion isochore (Fig. 8b, c). The calculated garnet composition at nucleation (the OS model) was then used to calculate the intersection of isopleths assuming equilibrium (the EQ model), as in Fig. 4. The resulting set of P–T points from the EQ model defines an array that trends downward in pressure and slightly upward in temperature (squares in Fig. 8b, c). The match is best for BC(b) (Fig. 8c), and both sets of calculations suggest the best correlation is with an overstepping of around 10 degrees and

0.6 kbar corresponding to around 2,000 J (per mole of garnet) affinity.

Staurolite–kyanite zone, eastern Vermont: sample TM-626a

A second sample from eastern Vermont is from the staurolite + kyanite zone approximately 4.4 km west of sample TM-549. X-ray maps (Fig. 9) and a line traverse (Fig. 10) reveal typical bell-shaped zoning of spessartine and minor zoning in almandine, pyrope, and grossular.

Raman spectra were collected from numerous quartz inclusions from several garnets on a thick (100 μm) sample of garnet separates (Table 4; Fig. 7b). The quality of the spectra obtained from sample TM-626a is significantly better than those from sample TM-549 (Fig. 7a) because the thick section allowed for larger inclusions to be measured. A range of wavelength shifts from 1.9 to 3.5 cm^{-1} was observed. Significantly, no difference in the maximum wavelength shift of 3.5 cm^{-1} was observed as a function of location in the garnet, that is, this maximum wavelength shift was observed in inclusions from both the core and the rim of the garnets. Whereas there are numerous ways that a quartz inclusion might record a lower internal pressure than that of entrapment (e.g., plastic deformation of the garnet or microcracks), it is difficult to envision how a quartz inclusion could record a higher pressure, so the maximum wavelength shift of 3.4–3.5 cm^{-1} is suspected to most accurately reflect the entrapment pressure. Nonetheless, results of calculations for a range of Raman shifts are presented (Fig. 11).

Figure 11 shows a simplified pseudosection for sample TM-626 and the results of calculations. The garnet core P–T conditions (red star) lie several tens of degrees above the equilibrium garnet isograd. As before, the QuiG barometry was used to constrain the locus of P–T conditions used to model overstepping (circles: the OS model).

Table 3 Measured core composition of garnet used for isopleth calculations (the EQ model)

	TM-549	TM-626	06MSF-6C[a]
Pyrope	0.058	0.066	0.056
Almandine	0.538	0.645	0.683
Spessartine	0.292	0.193	0.117
Grossular	0.112	0.096	0.144

[a] Analysis from Dragovic et al. (2012) recalculated with all Fe as FeO

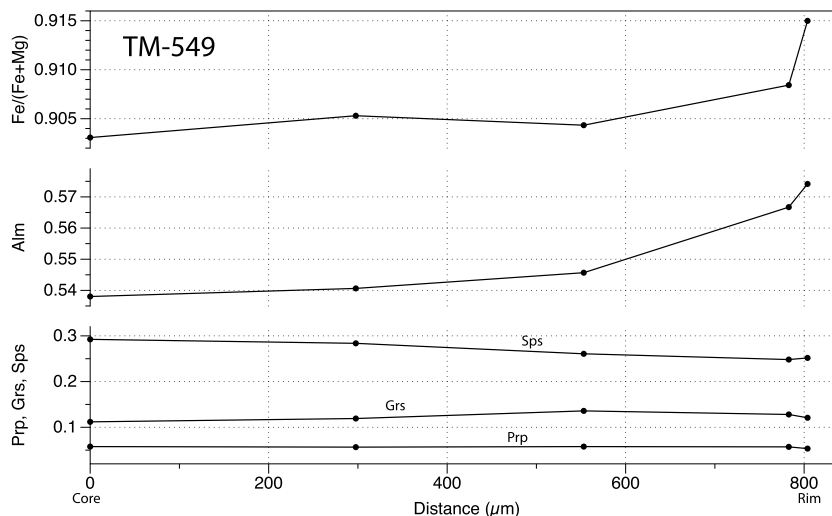**Fig. 6** Core-to-rim line traverses across garnet from sample TM-549 (Fig. 5)

Table 4 Measured Raman shifts and calculated internal pressure of quartz inclusions in garnet

Sample	Garnet crystal #	Quartz grain #	Spectrum	Raman shift (cm^{-1})[a]	Internal pressure (bars)[b]
TM-549	2	1	1	0.9	988
			2	1.1	1,209
			3	1.2	1,320
			4	1.1	1,209
			5	1.3	1,430
		3	1	1.1	1,209
		4	1	1.3	1,430
		5	1	1.3	1,430
		6	1	0.3	329
		7	1	−0.1	−109
		8	1	0.7	768
	3	1	1	0.8	878
			2	0.8	878
		2	1	1.0	1,099
		3	1	0.3	329
		4		0.2	219
TM-626	1	1	1	2.7	2,986
			2	2.7	2,986
			3	2.7	2,986
		2	1	1.9	2,095
		3	1	2.9	3,210
			2	3.0	3,322
		4	1	1.9	2,095
			2	2.0	2,206
		5	1	3.5	3,883
			2	3.4	3,770
	2	1	1	2.7	2,986
			2	2.5	2,763
		2	1	2.9	3,210
			2	2.9	3,210
			3	3.0	3,322
			4	3.0	3,322
			5	3.0	3,322

[a] Error on Raman shift is ±0.1 cm^{-1}

[b] Error on internal pressure is ±100 bars

For each set of OS model calculations, the P–T conditions calculated from the intersection of garnet isopleths assuming equilibrium (squares: the EQ model) are indicated by arrows. As with the previous calculations, the OS model garnet core compositions when used in the EQ model indicate P–T conditions for garnet formation that lie to lower pressures and temperatures than the true P–T conditions of nucleation.

The magnitude of the difference between the OS model and the EQ model calculated P–T conditions is quite large. All of the EQ model calculations of garnet core P–T conditions lie within 20 degrees of the equilibrium garnet isograd and are similar to the P–T conditions calculated from the actual garnet core composition (red star in Fig. 11). Significantly, the P–T conditions calculated from the actual garnet core (red star) lie 2–5 kbar below the pressure of garnet formation inferred from QuiG barometry.

Depending on which wavelength shift is assumed correct, the results in Fig. 11 suggest overstepping of as much as 50° and 5 kbar with affinities on the order of 10–18 kJ/mole garnet. Significantly, Menard and Spear (1994) report peak P–T conditions of a nearby sample (TM-590) of 8–9 kbar, 540–570 °C, raising the distinct possibility that nucleation of garnet in this sample was delayed to nearly peak metamorphic conditions were attained.

Blueschist facies, Sifnos, Greece

Dragovic et al. (2012) present a superb discussion of the petrogenesis of a sample of garnet–blueschist from Sifnos,

Fig. 7 Raman spectra of quartz inclusions in garnet from samples TM-549 (**a**) and TM-626a (**b**). *Colors* represent multiple spectra of individual grains identified by labels *Q1–Q5*. The *red lines* are spectra of matrix quartz, which is taken as the internal pressure = 1 bar baseline against which the shift of the inclusions is measured. Intensities of standard spectra (*red*) for the two samples were scaled by factors of 6 and 3, respectively, to fit in the graph
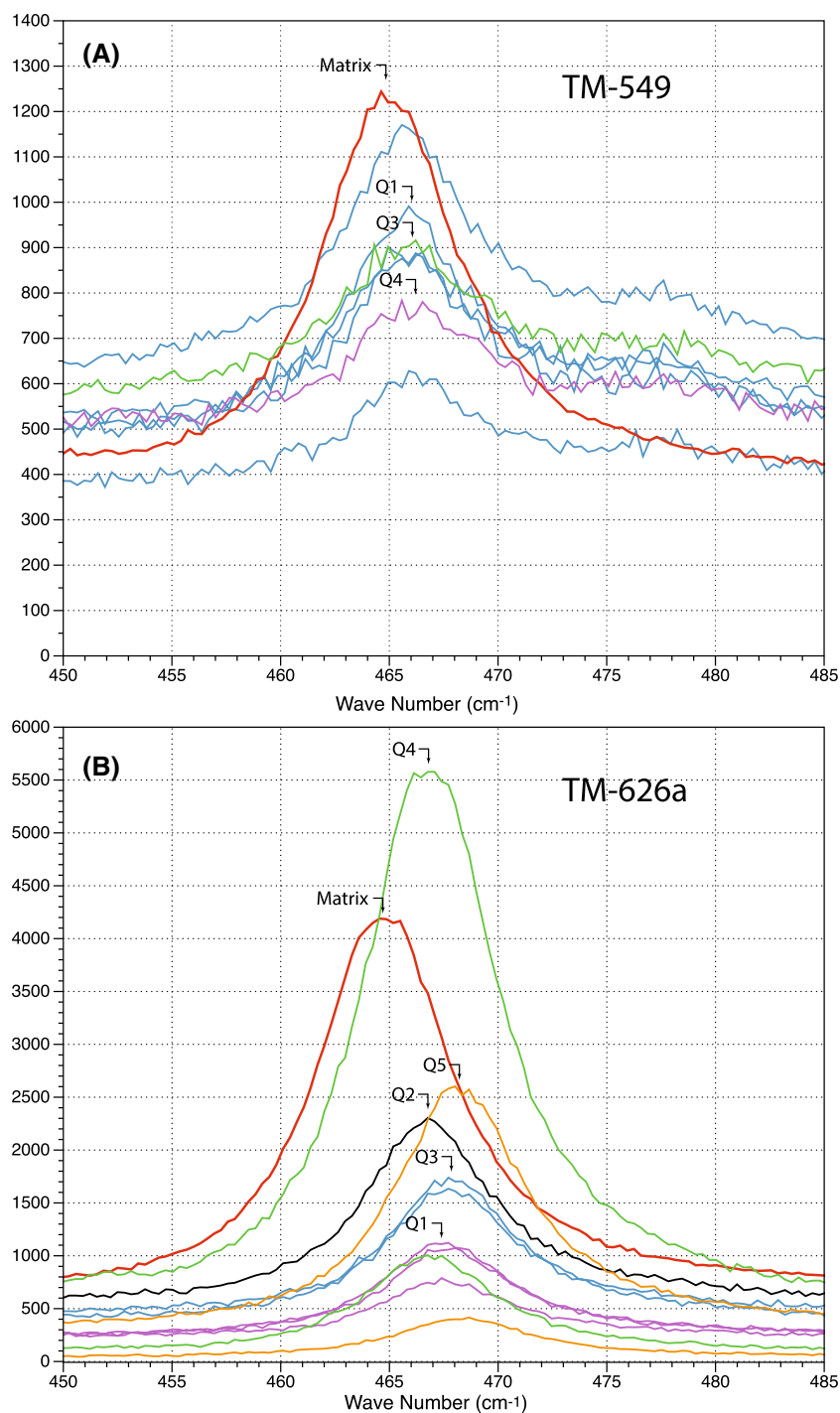
Greece, and the reader is referred to that paper for the details of the sample petrography. A sample from this area was also the subject of QuiG barometry by Ashley et al. (2014), and sufficient data are provided in these papers to conduct the type of analysis described above.

A simplified pseudosection for the whole-rock analysis of sample 06MSF-6C (Table 2) is presented in Fig. 12 along with calculations from this study. Also shown are the results of QuiG barometry using the thermoelastic model

and data suggested by Kohn (2014) and a maximum quartz wavelength shift for the core of garnet of 6.76 cm^{-1} as reported by Ashley et al. (2014). Three model OS calculations were done (circles in Fig. 12), and the P–T conditions were inferred from the intersection of garnet core isopleths computed from the EQ model (squares). It will be noticed that the inferred P–T conditions from the EQ model (squares) lie to lower temperature but higher pressure than the OS model P–T conditions (circles). This results again
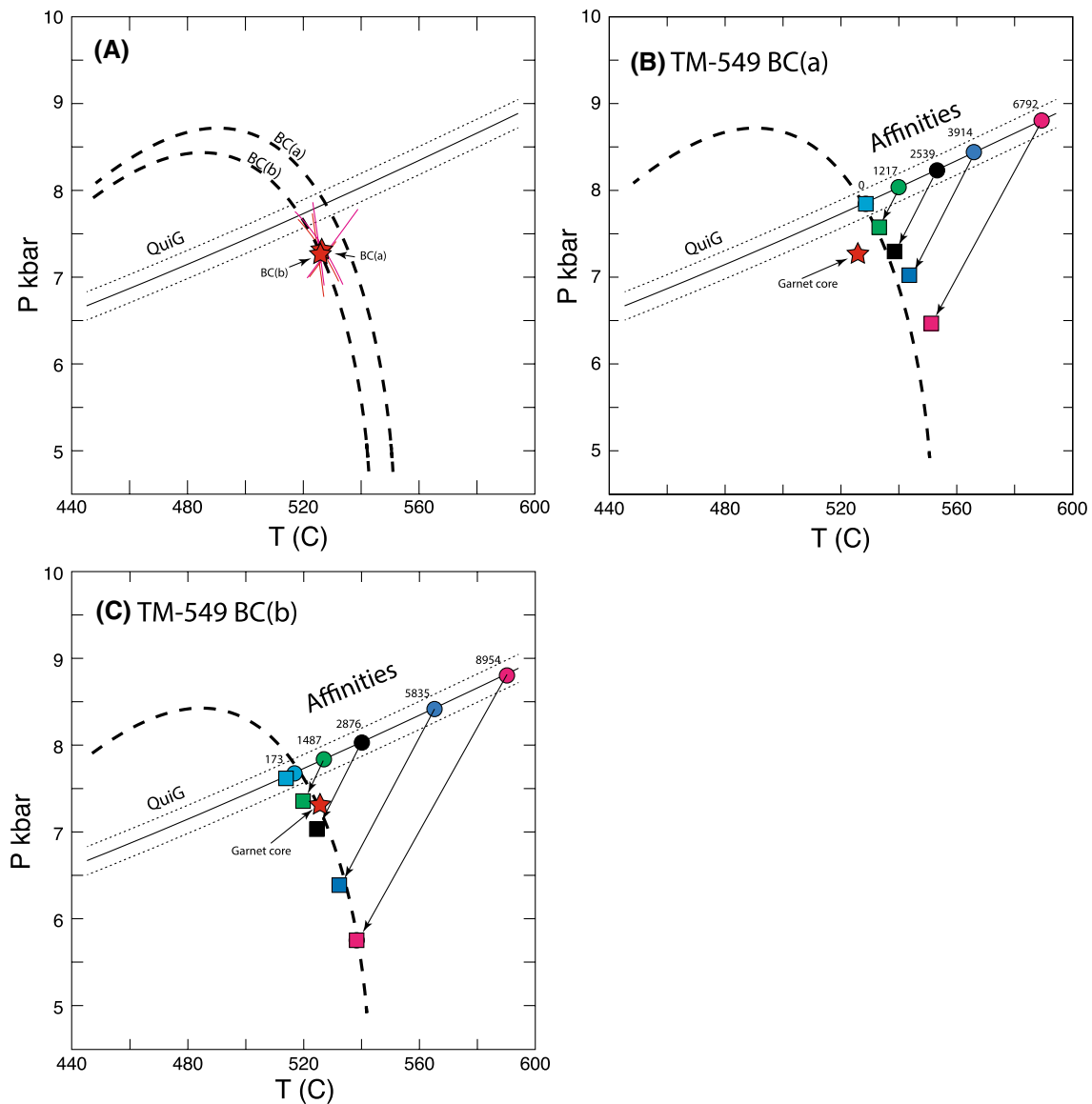
Fig. 8 P–T diagrams showing model results for sample TM-549. Line labeled QuiG is the result from quartz-in-garnet barometry, and dotted lines are ±1σ of the measurement of the maximum shift observed. **a** Calculated garnet isograd (*dashed lines*) for two bulk compositions (*BC(a)* and *BC(b)*) listed in Table 1. Also shown are the isopleth intersections for the garnet core composition for each bulk composition (*stars*: the EQ model). **b** Model results using *BC(a)*. *Circles* are the P–T conditions of the calculations for the OS model, *numbers* are affinities in joules/mole of garnet (12 oxygens), and arrows point to the isopleth intersection P–T conditions calculated from the model garnet nucleus composition (*squares*: the EQ model). **c** The same as in (**b**) using bulk composition *BC(b)*

because of the difference in spessartine and grossular contents of the OS model compared to the EQ model but equilibrium with lawsonite in the blueschist rather than plagioclase in the two examples above results in a higher rather than a lower apparent core pressure for the EQ model.

The P–T conditions implied by the measured garnet core composition (red star in Fig. 12) were also calculated using the EQ model after first recalculating all Fe in the garnet core analysis as FeO (e.g., no andradite component). There is a sizable triangle of uncertainty in the garnet isopleth

P–T conditions largely because of the low angle of intersection between the almandine and spessartine isopleths. Therefore, the preferred P–T conditions are those where almandine and spessartine intersect the grossular isopleth.

The P–T conditions inferred from the measured garnet core composition (red star) lie astride the garnet isograd for this bulk composition at a pressure approximately 1.5 kbar higher than the QuiG barometer. This discrepancy is within analytical uncertainty, and it could be concluded that very little overstepping was required for this garnet to nucleate.
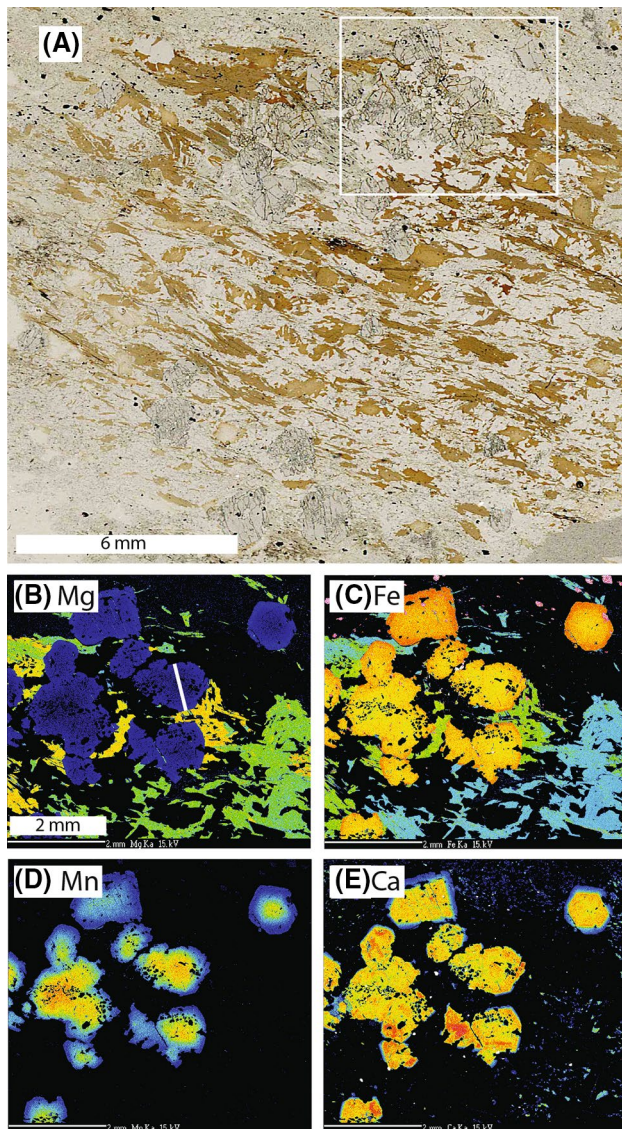
Fig. 9 Sample TM-626 (Latitude = 43.80450; Longitude = −72.33500). Staurolite–kyanite zone, eastern Vermont. **a** Photomicrograph showing biotite and garnet-rich layer. *Box* indicates the location of X-ray maps (**b–e**). X-ray maps of **b** Mg; **c** Fe; **d** Mn; and **e** Ca. *White line* in (**b**) shows the location of traverse (Fig. 10)

However, the results are equally consistent with overstepping of 80–90° (between the yellow and green circles at around 520–530 °C or around 9 kJ/mole garnet affinity). Most importantly, if significant overstepping occurred prior to nucleation of this garnet and subsequent growth occurred at the P–T conditions of nucleation or above, then the apparent P–T path followed by the sample (i.e., the path that one would infer from comparing core and rim P–T conditions assuming equilibrium growth) would be roughly one of nearly isobaric heating, as concluded by both Dragovic et al. (2012) and Ashley et al. (2014). However, had overstepping occurred then the garnet core

composition does not reflect equilibrium crystallization, and there is no information in the core composition about the conditions of core formation. Thus, the true P–T path followed by the rock to the peak (garnet rim) conditions is unknown. For example, a path of nearly isothermal loading to the peak P–T conditions would satisfy the observed chemistry equally well as one of isobaric heating. In fact, the texture of the sample suggests that very rapid garnet growth did occur, as would be expected from highly overstepped nucleation conditions. The garnet displays a honeycomb texture with numerous inclusions of quartz and, in other samples from the same locality in the authors' collection, honeycomb inclusions of pyroxene and epidote. In addition, Sm-Nd geochronology on garnet from this locality reported by Dragovic et al. (2012) indicates virtually no age difference between the core and the rim (46.50±.8 Ma for the core, 46.46±.59 for the rim), requiring rapid garnet growth (i.e., 0.04 Ma). Whereas extremely rapid heating is possible in a contact aureole, it is doubtful that such a rapid thermal excursion could occur in a subduction zone. Consequently, it is believed that a more reasonable interpretation is that garnet nucleation was overstepped by a considerable degree, presumably as a consequence of very rapid burial and that the garnet grew under nearly isothermal, isobaric conditions.

Discussion

Sample TM-549 requires only a modest degree of overstepping. This result is consistent with the observation that the sample was collected very near the mapped garnet isograd in the field. The garnets are small and did not grow appreciably after nucleation. The garnets also overgrow a crenulation cleavage, so it is possible that strain energy contributed to the energetics enabling garnet nucleation to occur with small degrees of overstepping.

The staurolite–kyanite zone and blueschist samples display similar results with respect to the degree of overstepping and both require on the order of 8 kJ/mole or higher garnet affinity. The implications of this result are profound for the study of metamorphic petrogenesis. Firstly, if overstepping has occurred, then there is no information preserved in the garnet zoning that can be used to reconstruct the prograde P–T path from equilibrium thermodynamic calculations. Indeed, one cannot rule out the possibility that the garnets studied grew isothermally and isobarically following nucleation. A thorough re-examination of what we believe to be true from metamorphic P–T path studies may be in order.

However, equally important is an appreciation of the tectonic perturbations that might give rise to significant overstepping. It is reasonable to conclude that, all other things

Fig. 10 Rim-to-rim line traverse across garnet from sample TM-626 (Fig. 9)
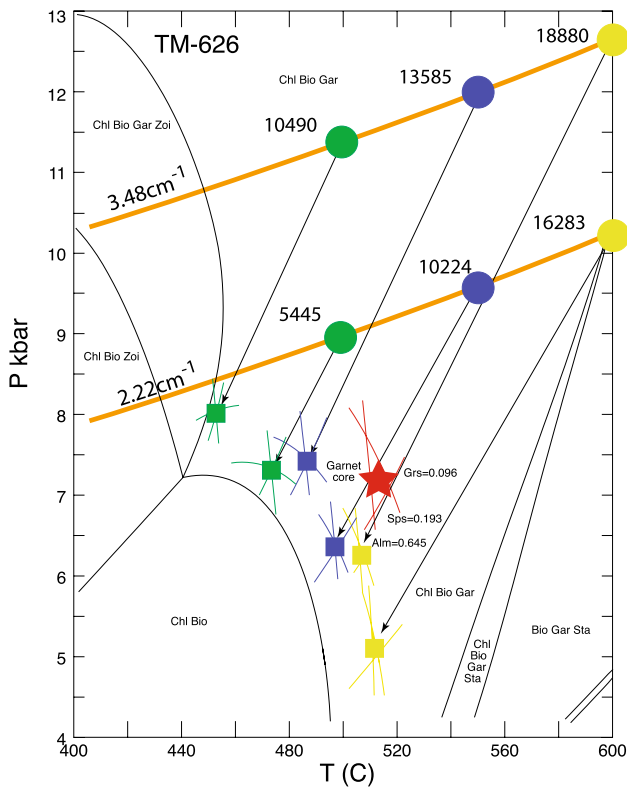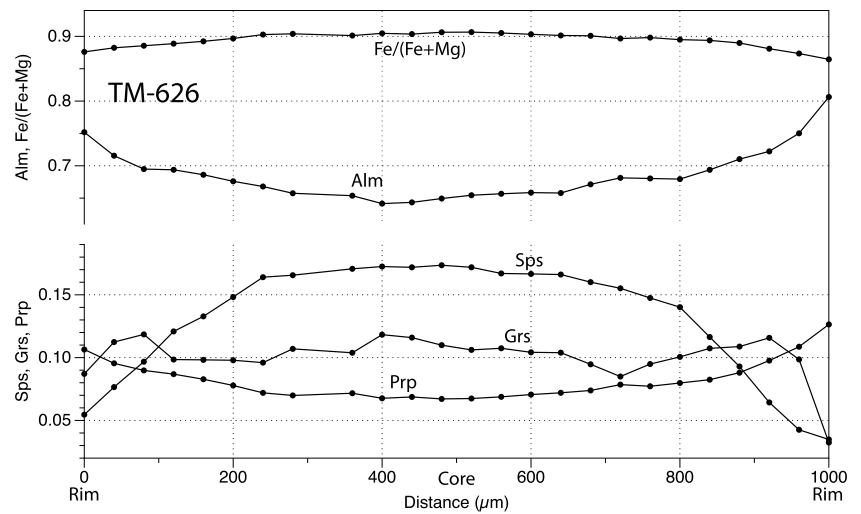

Fig. 11 P–T diagram showing a simplified pseudosection for the bulk composition of sample TM-626 (Table 1). *Orange lines* labeled 3.48 and 2.22 cm⁻¹ are calculated range of quartz entrapment conditions. *Red triangular* region with star labeled "Garnet core" is the intersection of isopleths of almandine, spessartine, and grossular for the garnet core (the EQ model). *Colored circles* are P–T conditions used for OS model calculations. *Labels* on circles are the affinity (joules/mole garnet). *Arrow* from each circle points to garnet nucleation isopleth intersections assuming equilibrium (*squares*: the EQ model). The calculations are most consistent with overstepping of several tens of degrees and 2–5 kbar
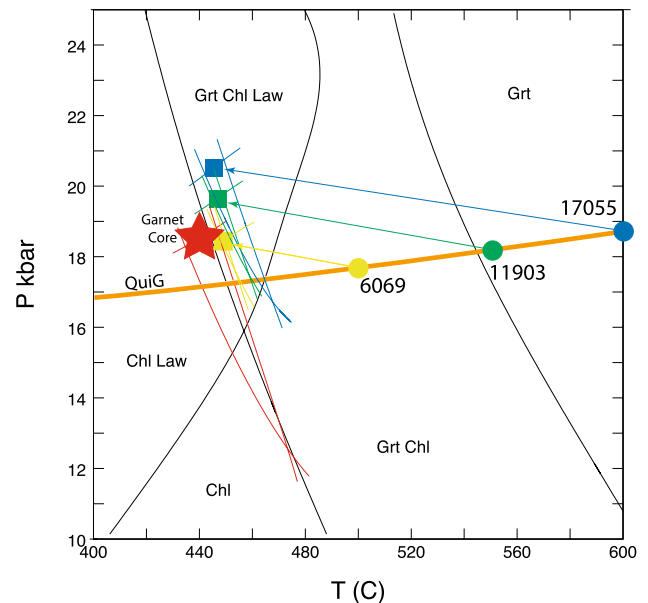

Fig. 12 P–T diagram showing a simplified pseudosection for the whole-rock bulk composition of sample 06MSF-6C (Dragovic et al. 2012). *Orange line* is the isochore of quartz entrapment based on the measurements of Ashley et al. (2014) and the authors' own measurement of similar samples from Sifnos. The *red star* labeled "Garnet core" is the intersection of isopleths of almandine + grossular and spessartine + grossular for the garnet core using analyses from Dragovic et al. (2012) recalculated assuming no ferric iron (the EQ model). *Colored circles* are conditions used for OS model calculations. *Labels* on circles are the affinity (joules/mole garnet). *Arrow* from each circle points to garnet nucleation isopleth intersections (*squares*) assuming equilibrium (the EQ model). The calculations are most consistent with garnet nucleation occurring along the isochore at around 520 °C (70° of overstepping) and an affinity of around 8,200 joules/mole garnet

being similar, significant overstepping is likely to be promoted by rapid changes in pressure and/or temperature. Although considerably more data are required to confirm the extent of overstepping in typical metamorphic terranes, it may turn out that rates of tectonic burial might be inferred through the analysis of the degree of overstepping. These types of studies could provide important new insights into the workings of the planet during crustal orogenesis.

References

Ashley KT, Caddick MJ, Steele-MacInnis MJ, Bodnar RJ, Dragovic B (2014) Geothermobarometric history of subduction recorded by quartz inclusions in garnet. Geochem Geophys Geosyst 15:350–360. doi:10.1002/2013GC005106

Dragovic B, Samanta LM, Baxter EF, Selverstone J (2012) Using garnet to constrain the duration and rate of water-releasing metamorphic reactions during subduction: an example from Sifnos, Greece. Chem Geol 314–317:9–22. doi:10.1016/j.chemgeo.2012.04.016

Enami M, Nishiyama T, Mouri T (2007) Laser Raman microspectrometry of metamorphic quartz: a simple method for comparison of metamorphic pressures. Am Mineral 92:1303–1315. doi:10.2138/am.2007.2438

Gaidies F, Pattison DRM, de Capitani C (2011) Toward a quantitative model of metamorphic nucleation and growth. Contrib Mineral Petrol 162:975–993. doi:10.1007/s00410-011-0635-2

Guiraud M, Powell R (2006) P–V–T relationships and mineral equilibria in inclusions in minerals. Earth Planet Sci Lett 244:683–694. doi:10.1016/j.epsl.2006.02.021

Hemley RJ (1987) Pressure dependence of Raman spectra of SiO_2 polymorphs: a-quartz, coesite, and stishovite. In: Manghnani MH, Syono Y (eds) High-Pressure Research in Mineral Physics. Terra Scientific, Tokyo/American Geophysical Union, Washington, pp 347–359

Kohn MJ (2013) "Geoba-Raman-try": calibration of spectroscopic barometers for mineral inclusions. Paper presented at the AGU 2013 fall meeting, San Francisco

Kohn MJ (2014) "Geoba-Raman-try": calibration of spectroscopic barometers for mineral inclusions. Earth Planet Sci Lett 388:187–196

Lasaga AC (1986) Metamorphic reaction-rate laws and development of isograds. Mineral Mag 50:359–373. doi:10.1180/Minmag.1986.050.357.02

Lasaga AC, Rye DM (1993) Fluid flow and chemical reaction kinetics in metamorphic systems. Am J Sci 293:361–404

Manning CE, Ingebritsen SE, Bird DK (1993) Missing Mineral Zones in Contact Metamorphosed Basalts. Am J Sci 293:894–938

Menard T, Spear FS (1994) Metamorphic P-T paths from calcic pelitic schists from the Strafford Dome, Vermont. J Metamorph Geol 12:811–826

Pattison DRM, Seitz JD (2012) Stabilization of garnet in metamorphosed altered turbidites near the St. Eugene lead–zinc deposit, southeastern British Columbia: equilibrium and kinetic controls. Lithos 134–135:221–235. doi:10.1016/j.lithos.2011.12.007

Pattison DRM, Tinkham DK (2009) Interplay between equilibrium and kinetics in prograde metamorphism of pelites: an example from the Nelson aureole, British Columbia. J of Metamorph Geol 27:249–279

Pattison DRM, De Capitani C, Gaidies F (2011) Petrological consequences of variations in metamorphic reaction affinity. J Metamorph Geol 29:953–977. doi:10.1111/j.1525-1314.2011.00950.x

Ridley J, Thompson AB (1986) The role of mineral kinetics in the development of metamorphic microtextures. In: Walther JV, Wood BJ (eds) Fluid-rock interactions during metamorphism. Springer, New York, pp 80–97

Rubie DC (1998) Disequilibrium during metamorphism: the role of nucleation kinetics. Geol Soc Spec Publ 138:199–214. doi:10.1144/Gsl.Sp.1996.138.01.12

Schmidt C, Ziemann MA (2000) In-situ Raman spectroscopy of quartz: a pressure sensor for hydrothermal diamond-anvil cell experiments at elevated temperatures. Am Mineral 85:1725–1734

Spear FS, Menard T (1989) Program GIBBS: a generalized Gibbs method algorithm. Am Mineral 74:942–943

Spear FS, Pyle JM (2010) Theoretical modeling of monazite growth in a low-Ca metapelite. Chem Geol 266:218–230

Spear FS, Peacock SM, Kohn MJ, Florence FP, Menard T (1991) Computer programs for petrologic P–T–t path calculations. Am Mineral 76:2009–2012

Walther JV, Wood BJ (1984) Rate and mechanism in prograde metamorphism. Contrib Miner Petrol 88:246–259

Waters DJ, Lovegrove DP (2002) Assessing the extent of disequilibrium and overstepping of prograde metamorphic reactions in metapelites from the Bushveld Complex aureole, South Africa. J Metamorph Geol 20:135–149. doi:10.1046/J.0263-4929.2001.00350.X

Wilbur DE, Ague JJ (2006) Chemical disequilibrium during garnet growth: Monte Carlo simulations of natural crystal morphologies. Geology 34:689–692. doi:10.1130/G22483.1

Zeh A, Holness MB (2003) The effect of reaction overstep on garnet microtextures in metapelitic rocks of the Ilesha Schist belt, SW Nigeria. J Petrol 44:967–994. doi:10.1093/Petrology/44.6.967